
Getting a-Round Guarantees: Floating-Point Attacks on Certified Robustness

Jiankai Jin, Olga Ohrimenko*, Benjamin I. P. Rubinstein*

School of Computing and Information Systems, The University of Melbourne

`jiankaij@student.unimelb.edu.au`

`oohrimenko@unimelb.edu.au`

`brubinstein@unimelb.edu.au`

Abstract

Adversarial examples pose a security risk as they can alter a classifier’s decision through slight perturbations to a benign input. Certified robustness has been proposed as a mitigation strategy where given an input x , a classifier returns a prediction and a radius with a provable guarantee that any perturbation to x within this radius (*e.g.*, under the L_2 norm) will not alter the classifier’s prediction. In this work, we show that these guarantees can be invalidated due to limitations of floating-point representation that cause rounding errors. We design a rounding search method that can efficiently exploit this vulnerability to find adversarial examples within the certified radius. We show that the attack can be carried out against several linear classifiers that have exact certifiable guarantees and against neural network verifiers that return a certified lower bound on a robust radius. Our experiments demonstrate over 50% attack success rate on random linear classifiers, up to 35% on a breast cancer dataset for logistic regression, and a 9% attack success rate on the MNIST dataset for a neural network whose certified radius was verified by a prominent bound propagation method. We also show that state-of-the-art random smoothed classifiers for neural networks are also susceptible to adversarial examples (*e.g.*, up to 2% attack rate on CIFAR10)—validating the importance of accounting for the error rate of robustness guarantees of such classifiers in practice. Finally, as a mitigation, we advocate the use of rounded interval arithmetic to account for rounding errors.

1 Introduction

Given the two computations:

$$((2 \times 10^{-30} + 10^{30}) - 10^{30}) - 10^{-30} ,$$

$$((-2 \times 10^{-30} + 10^{30}) - 10^{30}) + 10^{-30} ,$$

10^{-30} and -10^{-30} seem to be the obvious results [1]. However, due to rounding errors, the computed results on a machine with the IEEE 64-bit floating-point arithmetic [2] are -10^{-30} and 10^{-30} respectively. That is, one is underestimated because of rounding down, and one is overestimated due to rounding up.

Robustness of modern image classifiers has come under scrutiny due to a plethora of results demonstrating adversarial examples—small perturbations to benign inputs that cause models to mispredict, even when such perturbations are not evident to the human eye [3, 4, 5, 6]. If a learned model is used in critical applications such as self-driving cars, clinical settings or malware detection, such easily

*Authors made equal contributions to this work

added perturbations can have severe consequences. As a result, research focus has shifted to training models robust to adversarial perturbations, that come endowed with *provable certified robustness*.

Mechanisms for providing certified robustness aim to bound model misprediction rate given a certain level of perturbation. At a high level, such mechanisms return a radius R around x with a guarantee that for any x' within R distance from x (e.g., under the L_2 norm) $f(x) = f(x')$. How R is computed, whether it is sound and/or complete depends on the mechanism. For example, randomized smoothing [7, 8, 9] stabilizes a model’s predictions and uses Monte Carlo sampling to estimate a radius that with high-probability certified robustness. Bound propagation [10, 11], on the other hand, propagates the upper and lower bounds from the output layer to the input layer of a neural network, and gives a lower bound of the perturbation needed to flip the classification of the model. Misprediction rates can be further reduced by giving the classifier the rejection (abstain) option in the process of prediction. That is, a classifier can reject to make a prediction when it is not very confident [12, 13].

Given the extensive research on certifiable robustness in recent years, can such mechanisms protect against adversarial examples in practice? In this paper, we show that the limits posed by computer arithmetic invalidate guarantees of several prominent mechanisms and their implementations. Despite proofs of robustness guarantees on paper, they all assume that real numbers can be represented and manipulated exactly. Unfortunately, this critical (implicit) assumption cannot hold on computers with finite number representations. Since floating-point numbers can represent only a subset of real values, rounding is likely to occur when computing robust guarantees and can cause overestimation of the certified radius R . As a result, adversarial examples may exist within the computed radius despite claims of certification. In this paper:

- We introduce a new class of attacks that bypass certified robustness. Our attacks exploit rounding errors due to limited floating-point representation of real numbers.
- We devise a method for systematically finding such adversarial examples.
- We show that our attacks work against exact certifications of linear models [7], against a certified radius lower bound returned by a prominent neural network verifier [11]) on an MNIST-trained network, and against randomized certified robustness methods [7, 8] on neural networks for MNIST and CIFAR10. Our attack success rate differs between models and learners, reaching 50% for random linear classifiers and 9% on an MNIST neural network model—for both cases, in theory, the certification guarantees 0% attack success rate.
- We propose a defense based on rounded interval arithmetic, with strong theoretical and empirical support for mitigating attacks on linear models.

Related work. Besides integrity concerns regarding floating-point computation [1], attacks based on floating points have been used to invalidate privacy guarantees. For example, guarantees of differentially private mechanisms that use additive noise from continuous distributions such as Laplace or Gaussian are susceptible to attacks based on finite-precision representations of floating-point values [14, 15, 16]. Such attacks make an observation that certain floating points could not have been generated by a noise distribution algorithm. In another line of work, Andryscio *et al.* [17] exploit the difference in timing of floating-point arithmetic operations (e.g., multiplication by zero takes significantly less time than multiplication by a non-zero value) as a side-channel for information leakage in a differentially private system and a web-browser.

2 Background and preliminaries

We consider supervised learning on Euclidean vector spaces. Let input instance $x = (x_1, x_2, \dots, x_D)$ be a vector in \mathbb{R}^D with x_i denoting the component of x in the i th dimension. We adopt the L_2 norm $\|x\|_2 = \left(\sum_{i=1}^D |x_i|^2\right)^{1/2}$, written $\|x\|$ where the norm is understood from context, when measuring the length of instance vectors, and its induced metric $\|x - z\|$ for distances. We also use the L_1 norm $\|w\|_1 = \sum_{i=1}^D |w_i|$. We consider the task of learning a classifier f mapping an instance in \mathbb{R}^D to a label in $\{-1, 1\}$. Given a training set of N examples $(x^{(j)}, y^{(j)}) \in \mathbb{R}^D \times \{-1, 1\}$ drawn i.i.d. from some unknown distribution P , the goal of a learner \mathcal{A} is to output some classifier f with low risk $\mathbb{E}_P[\ell(f(X), Y)]$ for some loss $\ell(\cdot)$ of interest.

Linear models. We consider learners \mathcal{A} over two-class linear classifiers of the form $f(x) = \text{sign}(w^T x + b)$, for parameters $w \in \mathbb{R}^D$ the model weights and $b \in \mathbb{R}$ model bias. Specifically we consider as learners: (1) uniformly random sampling of (w, b) within a closed, bounded set, without consideration of training data; (2) the linear support vector machine that minimizes the L_1 -regularized squared hinge loss $\sum_{i=1}^n (1 - y^{(i)}(w^T x^{(i)} + b))_+^2 + \lambda \|w\|_1$; and (3) L_1 -regularized logistic regression that minimizes $\sum_{i=1}^n -\log p(y^{(i)} | x^{(i)}; w, b) + \beta \|w\|_1$ where labels are modelled as Bernoulli r.v.'s with $p(y = 1|x; w, b) = \sigma(w^T x + b)$, with $\sigma(z) = 1/(1 + \exp(-z))$ denoting the logistic or sigmoid function. While classifiers resulting from learners (1) and (3) directly make predictions as $f(x) = \text{sign}(w^T x + b)$, logistic regression's conventional classifier $f(x) = \text{sign}(\sigma(w^T x + b) - 0.5)$ is equivalent to this parameterization since $\sigma(\cdot) - 0.5$ preserves sign.

Neural networks. A feed-forward neural network forms output scores by composing a sequence of layers $F_i(\cdot)$ followed by a softmax (generalization of the logistic function to multiple classes): $F(x) = \text{softmax} \circ F_n \circ F_{n-1} \circ \dots \circ F_1$. The neural network forms its classification within classes $[K] = \{1, \dots, K\}$ by simple majority vote $f(x) = \arg \max_{k \in [K]} (F(x))_k$. Layers might take the form $F_i(x) = \sigma(\theta_i^T x) + \hat{\theta}_i$ for some weights θ_i and vector of model biases $\hat{\theta}_i$, convolutional layers for matrix- or tensor-valued inputs as is common for image data, max pooling, batch normalization, etc. The activation function σ may be the sigmoid (as defined above for logistic regression), tanh, ReLU, or otherwise. We consider convolutional neural networks involving convolutional, max pooling, and fully-connected layers, and ResNets that also use skip connections feeding inputs beyond two or three layers with batch normalization. Gradients of neural network outputs can be computed with respect to weights (for training) or inputs (for finding adversarial examples—see next) using backpropagation as typically implemented by reverse accumulation in autodiff libraries.

Adversarial examples. Given an input instance x , classifier f , and a target label $t \neq f(x)$, x' is a *targeted* adversarial example [5] if $f(x') = t$ where x' is reachable from x according to some chosen threat model. In the vision domain, it is common to assume that small L_p perturbations to x will go unnoticed by human observers. In this paper we consider L_2 distance, *i.e.*, $\|x - x'\| \leq \Delta$ for some small perturbation limit Δ . An adversarial example in the multi-class setting is *untargeted* if t is not specified, however, it is possible to find an x' such that $f(x') \neq f(x)$ while x' and x are still close. Appropriate methods for finding adversarial examples depend on the model under attack. For a two-class linear classifier f , its weight vector w is normal to the decision boundary $w^T x + b = 0$. Therefore, there always exists a closest adversarial example x' just beyond the decision boundary in the direction w . See Figure 1 for an illustration. For neural networks, and non-linear classifiers in general, the process is more involved. Two popular white-box approaches are due to Carlini and Wagner (C&W) [4] and Madry *et al.* called Projected Gradient Descent (PGD) [3]. These methods assume white-box access to the models (that is, access to architectures and model weights) and hence an attacker can run as many queries as they want and observe intermediate gradients on inputs of their choice. At a high level, PGD and C&W view a search for an adversarial example as an optimization problem where one tries to find x' with a flipped label while minimizing the distance to x , and differ in how the perturbation norm Δ is updated during the search.

2.1 Certified robustness

A robustness certification for a classifier at input x is a neighborhood of x on which classifier predictions are constant. Certifications aim to *guarantee that no small adversarial examples exist*. Typically neighborhoods are L_2 balls centered at x , while methods for certification may achieve a form of optimality (what we term completeness) in addition to correct certification (soundness).

Definition 1. A pointwise robustness certification for a K -class classifier f at input $x \in \mathbb{R}^D$ is a real radius $R > 0$ that is sound and (optionally) complete:

- (i) [sound] $\forall x' \in \mathbb{R}^D, \|x' - x\| \leq R \Rightarrow f(x') = f(x)$.
- (ii) [complete] $\forall R' > R, \exists x' \in \mathbb{R}^D, \|x' - x\| \leq R' \wedge f(x') \neq f(x)$.

A certification mechanism is any mapping from classifier and input to a candidate radius \tilde{R} (which may not be sound or complete). Where the computed radius $\tilde{R} \leq R$ for some sound radius R , it follows that \tilde{R} must also be sound. Outputting $\tilde{R} = 0$ is equivalent to abstaining from certification.

We categorize certification mechanisms in the literature depending on their specific claims.

<i>Exact mechanisms</i>	claim to output sound and complete radii.
<i>Conservative mechanisms</i>	claim to output sound radii that are not necessarily complete.
<i>Approximate mechanisms</i>	claim to output random radii that are sound (or abstain), with high probability $1 - \alpha$, and not necessarily complete.

Exact certification of linear classifiers. All linear (binary) classifiers $f(x) = w^T x + b$ admit a certified radius given by the straightforward expression $R = |w^T x + b| / \|w\|$. Cohen *et al.* derive this radius and prove its soundness [7, Proposition 4]— R is the distance from x to the decision boundary $w^T x + b = 0$ —and completeness [7, Proposition 5]—the projection of x onto the boundary is the closest point to x beyond which the class flips.

Conservative certification by bound propagation aims to provide a certified lower bound of minimum distortion [10, 11, 18, 19] to an input that would cause a label change. For neural networks, such methods maintain at each layer an outer approximation of the set of activation functions that are then used to derive an output bound for the network as a whole. There has been a significant amount of work in this space leading to support for several activation functions including ReLU and tanh, and a level of scalability.

Randomized smoothing for approximate certification. Researchers have extensively studied approximate certification of non-linear models such as neural networks, under the L_2 norm [9, 8, 7]. In this work, we consider two such approaches due to Li *et al.* [8] and Cohen *et al.* [7] from which many subsequent results derive. Sufficiently stable model predictions lead to certifiable radii; therefore we seek to stabilize the outputs of the base classifier f by forming a smoothed classifier g as follows. To input $x \in \mathbb{R}^D$ add isotropic Gaussian noise, then apply f . The input distribution induces a distribution over predictions: output the most likely class. That is, for $\epsilon \sim \mathcal{N}(0, \sigma^2 I^2)$,

$$g(x) = \arg \max_{k \in [K]} \Pr(f(x + \epsilon) = k) .$$

Here hyperparameter $\sigma > 0$ controls the level of smoothing: higher values lead to larger radii and higher risk. Consider lower (upper) bounds on the winning k^* (runner-up) classification’s probability score, $\Pr(f(x + \epsilon) = k^*) \geq p_A \geq \overline{p_B} \geq \max_{k \in [K] \setminus \{k^*\}} \Pr(f(x + \epsilon) = k)$. Then Cohen *et al.* prove that radius $R = 0.5\sigma(\Phi^{-1}(p_A) - \Phi^{-1}(\overline{p_B}))$ is a sound certification for smoothed classification $g(x)$. Note the authors prove that when applied to linear classifiers, this R recovers the sound and complete radius above. Several challenges arise when one wishes to apply these mechanisms to neural networks, relying, for example, on estimates for p_A and $\overline{p_B}$. Hence, the resulting certification R is then sound with high probability $1 - \alpha$ for a parameter of choice α . We elaborate on this and other challenges further in Appendix B.1.

3 Rounding search attack

We now present a rounding search method that exploits floating-point rounding errors to find adversarial perturbations within a computed certified radius.

Threat model. Like prior work on adversarial examples, we assume that the adversary has complete white-box access to a classifier f . Additionally, we assume that the adversary has white-box access to the certification mechanism $\tilde{R}(f, \cdot)$ that maps an input instance $x \in \mathbb{R}^D$ to a floating-point radius. When certification modifies a base classifier for predictions (*e.g.*, randomized smoothed \hat{g}) we take f to refer to the modified classifier—it is this classifier that forms predictions and certifications.

Key idea. Our attack builds on the following observation. Since there are floating-point rounding errors in the operations for computing a certification, the computed radius \tilde{R} at an instance x could overestimate a sound (and possibly complete) radius $R < \tilde{R}$. This creates leeway for an adversary to find adversarial perturbations whose norms are less than the computed certification radius, but which can change the classifications of the model, invalidating soundness of the certification.

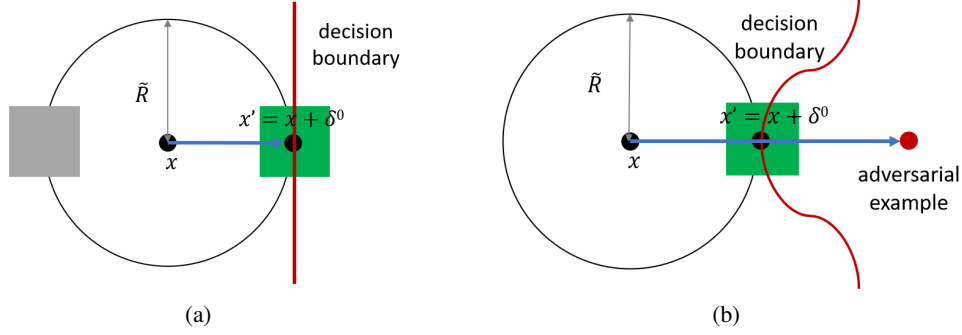


Figure 1: The search direction (blue line) and area (green area) for finding adversarial examples against machine learning models within robust radius \tilde{R} : (a) Linear model, whose decision boundary is a hyperplane, and the search direction equals model weights, w . (b) Neural network model, whose decision boundary is not evident, where we use gradients to find search direction using methods in [4, 3]. \tilde{R} is the computed certified radius, x is the original instance, δ^0 is the adversarial perturbation in the search direction, $x' = x + \delta^0$ is the seed for rounding search in the green area.

Baseline attack rates. We will conduct our rounding attack within floating-point approximations of the radius returned by exact, approximate and conservative methods. The baseline success rate for finding an adversarial example against a linear model within the radius defined in Section 2 should be 0% in theory, since the mechanism is exact: it claims to be both sound and complete. The baseline success rate for radii returned by conservative mechanisms should also be 0% since they too are claimed to be sound. Though randomized smoothing for neural networks comes with a failure rate $\alpha \ll 1$ to account for sampling error in approximating $g(x)$ by $\hat{g}(x)$ and in estimating confidence intervals towards computing \tilde{R} , it does not explicitly take into account errors due to rounding. Hence, we present success rates against these methods.

Floating-point representation. We now briefly describe how floating points are represented and then proceed to describing how we exploit rounding to construct adversarial examples. Floating-point values represent reals using three numbers: a sign bit b , an exponent e , and a significand $d_1 d_2 \dots d_d$. For example, 64-bit (double precision) floating-point numbers allocate 1 bit for b , 11 bits for e , and 52 bits for the significand. Such a floating-point number is defined to be $(-1)^b \times (1.d_1 d_2 \dots d_d)_2 \times 2^{e-1023}$. Floating points can represent only a finite number of real values. Hence, computations involving floating-point numbers often need to be rounded up or down to their nearest floating-point representation, as specified by the IEEE Standard for Floating-Point Arithmetic (IEEE 754). Rounding errors increase with the magnitude of the integer part of the number since the space between representable floating points increase with the integer part.

A naïve way to search for an adversarial example given classifier f , input x , computed radius \tilde{R} would be to try all x' such that $\|x - x'\| < \tilde{R}$, checking whether $f(x) \neq f(x')$. Unfortunately this exhaustive search is computationally intractable thanks to an tremendous number of floating points in the search space (*e.g.*, there are $\approx 2^{17}$ floating points in a small interval such as $[10, 10 + 2^{-32}]$).

For linear models, we can avoid futile search with the observation that instances in the gray area, as depicted in Figure 1, cannot possibly flip predictions, as they are in the opposite direction of the decision boundary. Direction $d = w$ is normal to the boundary’s hyperplane $w^T + b = 0$; it is this direction that reaches the decision boundary in the shortest distance.

The perturbation direction for neural networks is not as obvious as it is for linear models given their complex structure (*e.g.*, see Figure 1 for an illustration). We therefore resort to local search guided by gradients and adopt two prominent attack methods in our experiments: C&W [4] and PGD [3]. These attacks use gradients to optimize change in classifier prediction score w.r.t. perturbation direction d . With the perturbation direction d and the certified radius \tilde{R} , we select our perturbation search seed as

$$\delta^0 = \frac{\tilde{R}}{\|d\|} d = \frac{\tilde{R}}{\|x' - x\|} (x' - x) , \quad (1)$$

where x' is the adversarial example as found by *e.g.*, PGD or C&W, corresponding to perturbation $d = x' - x$. We then search around δ^0 for neighbors δ' with norms that are “just” smaller than \tilde{R} , and which can change model classification. (See Figure 1 for an illustration.)

Neighbors δ' are sampled using the neighboring floating-point values of the components of D -dimensional δ^0 . For example, the floating points before and after 1.0 are 0.9999999999999999 and 1.0000000000000002 respectively, for the IEEE 64-bit representation. For a $\delta^0 = (1.0, 1.0)$, its neighbors δ' could be $(0.9999999999999999, 1.0)$, $(1.0, 1.0000000000000002)$, and so on.

The total number of neighbors N grows exponentially with the dimension D of the input. For example, for every dimension i , the adversary can choose to check the first n neighboring values smaller and the first n neighboring values larger than the value of δ_i^0 . Since there are $2n + 1$ values that each δ_i^0 can be set to, there are $N = (2n + 1)^D$ possibilities for δ' . We use n as a parameter of the search (*e.g.*, in our experiment, we set $n = 2$, hence $N = 5^D$). If N is too high we propose a randomized approach where we uniformly sample $N' \ll N$ neighbors.

For every δ' we choose, we check for $\|\delta'\| \leq \tilde{R}$ and $f(x) \neq f(x + \delta')$. If any δ' satisfies those two conditions simultaneously, we say that our attack is successful for this x .

4 Attack experiments

In this section, we evaluate whether our rounding search attacks can find adversarial examples within a certified radius. We first consider several learners of linear classifiers, including logistic regression and the linear support vector machine (SVM). The *exact* certified radius for a binary linear classifier is $R = |w^T x + b|/\|w\|$ [7] (Section 2). We then consider a neural network model, whose certified radius is obtained through bound propagation [11]—an exemplar of *conservative certification*. We show that our rounding search finds adversarial examples within radii for both of these mechanisms. Recall that the baseline success rate for finding an adversarial example against such mechanisms should be 0% in theory, as such mechanisms claim to be *sound*. Finally, we also present attack success rate against *approximate* mechanisms [8, 7] that certify neural networks with high probability.

All our linear models are run on an Intel Xeon Platinum 8180M CPU, while our neural network learners and models are run on a Tesla V100 GPU.

4.1 Random linear classifiers

To evaluate the performance of our attack in an ideal scenario, we first conduct our attack on randomly initialized (binary) linear classifiers with randomly generated target instance:

$$f(x) = \text{sign}(w^T x + b) ,$$

where weights w_i and bias b_i are random values drawn from a range $[-1, 1]$, $\forall i \in [D] = \{1, \dots, D\}$, and D ranges in $[100]$. Each value is represented with 32-bit or 64-bit floating-point precision. For each dimension, we test 10,000 randomly initialized models. For each model we choose one instance x to attack, where each component x_i is drawn randomly from $[-1, 1]$. Hence, attack success rate measures the number of models out of 10,000 for which a random instance can result in an attack. For a test on each combination of (w, b, x) , we evaluate $N' = D^2$ randomly chosen samples in the search area with $n = 2$ (*i.e.*, $N = 5^D$). Note that since the number of neighbors increases exponentially with D , we also increase the number of samples we evaluate.

Results are shown in Figure 2(a). With higher dimension, our attack success rate first increases and then flattens around 50%. Recall that with higher dimension more arithmetic operations are done in computing $\|\delta'\|$ and \tilde{R} , which results in accumulation of rounding errors and a higher total rounding error. Hence, the attack success rate increases. To demonstrate this phenomenon further, we measure maximum rounding error across $D \in \{20, \dots, 1000\}$ and report the correlation between the two in Figure 2(b). N' grows slower than N , so the sampled neighbors will be diluted in the search area when the dimension gets higher, that is, a smaller proportion of potential neighbors δ' in the search area will be evaluated, thus our success rate flattens.

The attack success rates appear to be the same when all computation is done either within 32-bit or 64-bit precision. That is, rounding is affecting all computations equally in our attack.

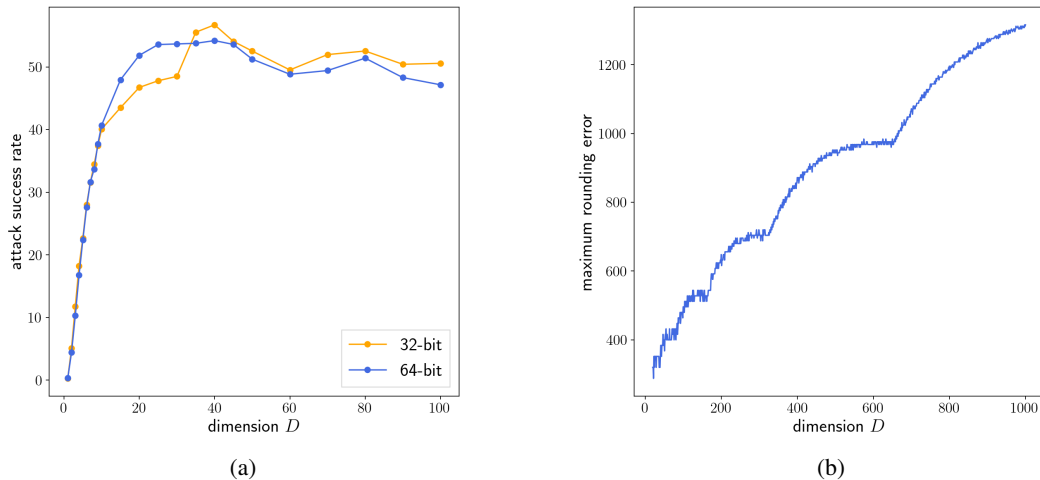


Figure 2: (a) Rounding search attack success rates against a random binary linear classifier. For each dimension D , we report the number of 10,000 randomly initialized models for which we can successfully find an adversarial example within certified radius \tilde{R} for a random example x drawn from $[-1, 1]^D$. Since the attacks are against an exact certified radius, the baseline attack rate should be 0. Model weights w and biases b are randomly initialized with $w \in [-1, 1]^D$, $b \in [-1, 1]$. We use two settings to represent the values: all values and computation is done using 32-bit floating points (FPs) or 64-bit FPs. (b) Maximum rounding error in the calculation of the certified radius \tilde{R} on a sample x with each $x_i = 3.3 \times 10^9$, for the linear model with $w_i = 3.3 \times 10^{-9}$, $b = 3.3 \times 10^9$, where $i \in [1, D]$ and $D \in [20, 1000]$. Results for $D \in [1, 20)$ are not included since division when computing \tilde{R} overflows when $D < 20$.

4.2 Logistic regression and linear SVM

In this section, we evaluate our attack on models trained with real datasets.

Breast cancer Wisconsin dataset. We now evaluate our rounding search attack on the logistic regression (LR) and linear SVM classifiers on the Breast Cancer Wisconsin (BCW) dataset [20], with 341 records used for training, and 228 records for validation and evaluation of our attacks. There are 30 attributes (*i.e.*, $D = 30$) in the dataset and we assume there are no domain constraints on these attributes. We trained LR with the stochastic gradient descent optimizer, and (primal) linear SVM using sequential minimal optimization. The validation accuracy of LR for the BCW dataset is 86.4% and 97.8% for linear SVM. We then try to find an adversarial example w.r.t. each example in the test dataset. The rounding search evaluates $N' = 5,000$ randomly chosen samples in the search area per test instance. We obtain attack success rates of 35.1% and 25.9% for LR and linear SVM models, respectively. Since we select only those adversarial examples whose perturbation is within the certified radius by an exact mechanism, the baseline attack success rate is 0%.

MNIST dataset. MNIST [21] dataset contains images of hand-written digits where each image has 784 attributes and each attribute is a pixel within the domain $[0, 255]$. We used around 12000 images for training, and around 2000 images for validation and evaluation of our attacks, for each combination of the labels $i, j \in \{0, \dots, 9\}$. The constraint on the domain restricts the space of adversarial examples since a simple filter would be able to detect such examples. We train LR and linear SVM models on MNIST similar to the training process for BCW with the exception of adding L_1 regularization that ensures that model weights are sparse. For each classifier, we trained 45 models for each combination of the labels $i, j \in \{0, \dots, 9\}$ of the MNIST dataset. Validation accuracies range between 60% and 70% for LR and between 91% and 99% for linear SVM.

We observed non-zero attack success rate for 22/45 and 31/45 models for LR and linear SVM, respectively (full results appear in the appendix in Tables 1 and 2). For these models attack success are in the ranges $[0.1\%, 3.43\%]$ and $[0.1\%, 11.05\%]$, respectively. Though these results may seem

low at a first glance, we remind the reader that they should be 0% as perturbations in all these adversarial examples are within the certified radius. We demonstrate several original and adversarial images together with their perturbation and certified radius information in Figure 3 of the appendix.

4.3 Neural network certification with β -Crown

We now turn our attention to neural networks and mechanisms whose certification guarantees are sound but not complete. That is, they provide a lower bound on the radius and it is possible that a tighter radius may exist. We use β -Crown verifier with branch and bound method on the 4-layer CNN model for MNIST as defined and implemented in [11], with perturbation size $\Delta = 0.3$ in the L_2 metric. Using bound propagation this method returns a lower bound on the distortion to x that would flip the classification of the model to another class (e.g., the runner-up class). We conduct our rounding search attack on the first 1,000 examples from the MNIST test dataset that have been verified against their runner-up class.

We use PGD [3, 22] to find the perturbation $d = x' - x$. Our PGD iterates for 50 times at most, with step size $\Delta/10$. Δ is our perturbation limit, and is set as the certified radius \tilde{R} as returned by the verifier for x . If the perturbation norm $\|d\|$ is smaller than \tilde{R} , then we take x' as a successful attack directly. Otherwise, if $\|d\|$ is larger than \tilde{R} , we scale the perturbation as in Equation (1), and run our rounding search. If the search finds at least one adversarial example that is classified as the runner-up class, success is returned for x .

We observe that the original PGD is successful only 0.9% of the time, while the rounding attack has success rate of 8.7%. We note that it is already surprising that even PGD is successful. We hypothesize that this could be due to rounding errors that are accumulated during bound propagation process of β -Crown which involves many computations involving floating points. Our attack can exploit rounding errors further by ensuring that search is performed by small perturbations to the inputs next to a decision boundary.

4.4 Approximate certification

In this section, we consider approximate certification methods based on randomized smoothing and evaluate their susceptibility to rounding attacks. We use certified radii established in [7] and [8], which we refer to as R_C and R_L respectively. Recall that randomized smoothing guarantees are probabilistic and have a failure probability. The failure arises due to the limited number of Monte Carlo samples (i.e., predictions on noise-corrupted examples) used in the estimation of the certified radius. Nevertheless we report a summary of our results here and refer the reader to Appendix B.2.

We use MNIST [21] and the CIFAR10 [23] datasets, with the same network architecture and data preprocessing procedures as [4, 7]. As recommended in the papers on radii R_C and R_L , we set the error rate to $\alpha = 0.1\%$.

Within R_C and R_L , our rounding attacks have up to 1.3% attack success rate on the MNIST dataset, and have up to 2.2% attack success rate on the CIFAR-10 dataset. Attack success rates within radius R_C are slightly higher than attack success rates within R_L , possibly due to the estimation method by Li *et al.* being more conservative than the one by Cohen *et al.* (See Figure 6 of the appendix for a comparison.) We note that one should consider above non-zero attack results carefully since both certified methods fall under approximate methods and have a failure rate of 0.1%. The goal of our experiments is to show that adversarial examples within R are possible and error rate should be reported and taken into account by practitioners when building systems that rely on these guarantees.

5 Mitigation: Certification with rounded interval arithmetic

Our attack results demonstrate that inappropriate floating-point rounding invalidates the soundness claims of a wide range of certification mechanisms implementations for a variety of common learners and models. We now outline a mitigation that uses rounded interval arithmetic, a technique from numerical analysis typically used for bounding numerical stability in scientific computing [24].

While the default rounding mode in the IEEE 754 floating-point arithmetic standard [2] is round-to-nearest, one can instruct an IEEE 754 compliant system to round down or up. Judicious use of these

rounding modes is critical to computing sound certifications. To lower bound a real radius $R \geq \tilde{R}$ one might intuit that each operation towards \tilde{R} should *always* be rounded down, however this is not the case. Consider intermediate computation $c := a - b$ where real $a - b$ cannot be represented as a floating point. If a, b were elementary floating-point values then rounding down would guarantee c lower bounds (real) $a - b$. However to lower bound real $d - c = d - (a - b)$, we require an upper bound on real $a - b$ for subtracting from d , not a lower bound. Rounded interval arithmetic addresses this issue by replacing every numerical value with an interval.

Interval operators exist for elementary arithmetic operations, for example: for real intervals $[a_1, a_2], [b_1, b_2]$

- Addition is defined as $[a_1 + b_1, a_2 + b_2]$.
- Subtraction is defined as $[a_1 - b_2, a_2 - b_1]$.
- Multiplication is defined as $[\min\{a_1b_1, a_2b_1, a_1b_2, a_2b_2\}, \max\{a_1b_1, a_2b_1, a_1b_2, a_2b_2\}]$.

For real arithmetic operator $*$, its interval arithmetic operator extension guarantees a resulting interval I containing $a * b$ for all $a \in [a_1, a_2], b \in [b_1, b_2]$ —Definition 2 extends this property to M -ary operators. Rounded interval arithmetic further employs rounding down (up) for the lower (upper) interval limit to make the same guarantee for floating point. By representing constants as singleton intervals, so for example, rounded interval arithmetic computes floating-point bounds on real results: $[1, 1]/[3, 3] = [0.3333333333333333, 0.3333333333333337]$. Interval variants exist for all standard mathematical functions. For example, the square root is efficiently implemented via an interval Newton method [25]. The following result describing our mitigation strategy is proved in Appendix C.

Definition 2. We call an M -ary operator ϕ mapping sequences of M floating-point intervals to a floating-point interval, a *sound floating-point extension* of an M -ary operator ψ mapping M reals to a real, if for any floating-points, $a_1^{(1)}, a_2^{(1)}, \dots, a_1^{(M)}, a_2^{(M)}$ and any reals a_1, \dots, a_M , if $\forall i \in [M], a_i \in [a_1^{(i)}, a_2^{(i)}]$ then $\psi(a_1, \dots, a_M) \in \phi\left(\left([a_1^{(1)}, a_2^{(1)}], \dots, [a_1^{(M)}, a_2^{(M)}]\right)\right)$.

Lemma 1. Consider a classifier f , D -dimensional floating-point instance x , and a certification mechanism $R(f, x)$ that is sound when employing real arithmetic. If $R(f, \cdot)$ can be computed by a composition of real-valued operators ψ_1, \dots, ψ_L with sound floating-point extensions ϕ_1, \dots, ϕ_L , then the following certification mechanism $\underline{R}(f, x)$ is sound with floating-point arithmetic: run the compositions of ϕ_1, \dots, ϕ_L on intervals $[x, x], [f(x), f(x)]$ to obtain $[\underline{R}, \bar{R}]$; return \underline{R} .

We used the PyInterval library [26] that performs rounded interval arithmetic to compute sound \underline{R} for linear classifiers [7], using the above addition and multiplication operators, rounded interval division, and interval Newton-based square root. Our attack success rates for randomly initialized linear classifiers (Section 4.1) drop to 0% uniformly for all dimensions. In sum, our theoretical and empirical results provide strong support for mitigating attacks against exact robustness certifications [7].

Bound propagation employed in conservative certifications [10, 11, 18, 19] closely resembles interval arithmetic—it is plausible that incorporation of rounded interval arithmetic could mitigate accumulation of round errors in corresponding neural network certifications. Randomized smoothing [7, 8] presents additional questions: while base classifier $f(\cdot)$ may not require rounded interval arithmetic, estimation $\hat{g}(x)$ of $g(x)$ almost certainly would; and effects of floating-point Gaussian sampling may also require modification of final certification.

6 Conclusion

Certified robustness has been proposed as a defense against adversarial examples that can change model prediction through small input perturbations. In this work we have shown that guarantees of several certification mechanisms do not hold in practice since they rely on real numbers that are approximated on modern computers. Hence, computation on floating-point numbers—used to represent real numbers—can overestimate certification guarantees due to rounding. We propose and evaluate a search method that finds adversarial inputs on robust linear classifiers and a verified neural network within their certified radii—violating their certification guarantees. We propose rounded interval arithmetic as the mitigation, by accounting for the rounding errors involved in the computation of certification guarantees. We conclude that if certified robustness is to be used for

security-critical applications, their guarantees and implementations need to account for limitations of modern computing architecture.

7 Acknowledgment

This work was supported by the joint CATCH MURI-AUSMURI, and The University of Melbourne’s Research Computing Services and the Petascale Campus Initiative. The first author is supported by the University of Melbourne research scholarship (MRS) scheme.

References

- [1] Ulrich W Kulisch and Willard L Miranker. The arithmetic of the digital computer: A new approach. *Siam Review*, 28(1):1–40, 1986.
- [2] IEEE standard for floating-point arithmetic. *IEEE Std 754-2019 (Revision of IEEE 754-2008)*, pages 1–84. doi: 10.1109/IEEESTD.2019.8766229.
- [3] Aleksander Madry, Aleksandar Makelov, Ludwig Schmidt, Dimitris Tsipras, and Adrian Vladu. Towards deep learning models resistant to adversarial attacks. *arXiv preprint arXiv:1706.06083*, 2017.
- [4] Nicholas Carlini and David Wagner. Towards evaluating the robustness of neural networks. In *IEEE Symposium on Security and Privacy (S&P)*, pages 39–57, 2017.
- [5] Christian Szegedy, Wojciech Zaremba, Ilya Sutskever, Joan Bruna, Dumitru Erhan, Ian Goodfellow, and Rob Fergus. Intriguing properties of neural networks. In *International Conference on Learning Representations (ICLR)*, 2014. URL <http://arxiv.org/abs/1312.6199>.
- [6] Ian Goodfellow, Jonathon Shlens, and Christian Szegedy. Explaining and harnessing adversarial examples. In *International Conference on Learning Representations (ICLR)*, 2015. URL <http://arxiv.org/abs/1412.6572>.
- [7] Jeremy Cohen, Elan Rosenfeld, and Zico Kolter. Certified adversarial robustness via randomized smoothing. In *International Conference on Machine Learning (ICML)*, pages 1310–1320. PMLR, 2019.
- [8] Bai Li, Changyou Chen, Wenlin Wang, and Lawrence Carin. Certified adversarial robustness with additive noise. In *Conference on Neural Information Processing Systems (NeurIPS)*, volume 32, 2019.
- [9] Mathias Lecuyer, Vaggelis Atlidakis, Roxana Geambasu, Daniel Hsu, and Suman Jana. Certified robustness to adversarial examples with differential privacy. In *IEEE Symposium on Security and Privacy (S&P)*, pages 656–672, 2019.
- [10] Huan Zhang, Tsui-Wei Weng, Pin-Yu Chen, Cho-Jui Hsieh, and Luca Daniel. Efficient neural network robustness certification with general activation functions. In *Conference on Neural Information Processing Systems (NeurIPS)*, volume 31, 2018.
- [11] Shiqi Wang, Huan Zhang, Kaidi Xu, Xue Lin, Suman Jana, Cho-Jui Hsieh, and J Zico Kolter. Beta-CROWN: Efficient bound propagation with per-neuron split constraints for complete and incomplete neural network verification. *Conference on Neural Information Processing Systems (NeurIPS)*, 34, 2021.
- [12] Jiefeng Chen, Jayaram Raghuram, Jihye Choi, Xi Wu, Yingyu Liang, and Somesh Jha. Revisiting adversarial robustness of classifiers with a reject option. In *The AAAI-22 Workshop on Adversarial Machine Learning and Beyond*, 2021.
- [13] Kenneth Hung and William Fithian. Rank verification for exponential families. *The Annals of Statistics*, 47(2):758–782, 2019.
- [14] Ilya Mironov. On significance of the least significant bits for differential privacy. In *ACM Conference on Computer and Communications Security (CCS)*, 2012.

- [15] Jiankai Jin, Eleanor McMurtry, Benjamin I.P. Rubinstein, and Olga Ohrimenko. Are we there yet? timing and floating-point attacks on differential privacy systems. In *IEEE Symposium on Security and Privacy (S&P)*, 2022.
- [16] Naoise Holohan and Stefano Braghin. Secure random sampling in differential privacy. *CoRR*, abs/2107.10138, 2021. URL <https://arxiv.org/abs/2107.10138>.
- [17] Marc Andryscio, David Kohlbrenner, Keaton Mowery, Ranjit Jhala, Sorin Lerner, and Hovav Shacham. On subnormal floating point and abnormal timing. In *IEEE Symposium on Security and Privacy (S&P)*, pages 623–639. IEEE Computer Society, 2015. doi: 10.1109/SP.2015.44. URL <https://doi.org/10.1109/SP.2015.44>.
- [18] Eric Wong and Zico Kolter. Provable defenses against adversarial examples via the convex outer adversarial polytope. In *International Conference on Machine Learning (ICML)*, pages 5286–5295. PMLR, 2018.
- [19] Shiqi Wang, Kexin Pei, Justin Whitehouse, Junfeng Yang, and Suman Jana. Formal security analysis of neural networks using symbolic intervals. In *USENIX Security Symposium*, pages 1599–1614, 2018.
- [20] Dheeru Dua and Casey Graff. UCI machine learning repository, 2017. URL <http://archive.ics.uci.edu/ml>.
- [21] Yann LeCun, Corinna Cortes, and CJ Burges. Mnist handwritten digit database. *ATT Labs [Online]*. Available: <http://yann.lecun.com/exdb/mnist>, 2, 2010.
- [22] Nicolas Papernot, Fartash Faghri, Nicholas Carlini, Ian Goodfellow, Reuben Feinman, Alexey Kurakin, Cihang Xie, Yash Sharma, Tom Brown, Aurko Roy, et al. Technical report on the cleverhans v2. 1.0 adversarial examples library. *arXiv preprint arXiv:1610.00768*, 2016.
- [23] Alex Krizhevsky. Learning multiple layers of features from tiny images. Technical report, 2009.
- [24] Nicholas J. Higham. *Accuracy and stability of numerical algorithms*. SIAM, 2002.
- [25] Eldon Hansen and G. William Walster. *Global optimization using interval analysis: revised and expanded*, volume 264. CRC Press, 2003.
- [26] S Taschini. PyInterval, interval arithmetic in Python, 2008.
- [27] Lawrence D Brown, T Tony Cai, and Anirban DasGupta. Interval estimation for a binomial proportion. *Statistical science*, 16(2):101–133, 2001.

A Attack results on MNIST for logistic regression and linear SVM

Table 1: The success rates of our rounding search attack against LR models on the MNIST dataset, with perturbation $\|\delta\| < R$ where $R = |w^T x + b|/\|w\|$. 45 LR models have been trained and attacked for each combination of labels $i, j \in [10]$. We use - to denote models where rounding search did not find an adversarial example. Recall that the baseline attack success rate should be zero when the radius is certified exactly.

Labels	1	2	3	4	5	6	7	8	9
0	0.38%	0.84%	0.05%	0.76%	0.64%	-	2.99%	3.43%	-
1		-	-	2.65%	2.17%	0.24%	0.88%	-	2.99%
2			-	0.1%	0.1%	-	-	-	0.05%
3				-	0.26%	-	-	0.05%	-
4					-	0.1%	-	-	0.05%
5						-	-	-	-
6							-	0.31%	0.25%
7								0.2%	-
8									-

Table 2: The success rates of our rounding search attack against linear SVM models on the MNIST dataset, with perturbation $\|\delta\| < R$ where $R = |w^T x + b|/\|w\|$. 45 linear SVM models have been trained and attacked for each combination of labels [10]. We use - to denote models where rounding search did not find an adversarial example. Recall that the baseline attack success rate should be zero when the radius is certified exactly.

Labels	1	2	3	4	5	6	7	8	9
0	-	0.94%	0.15%	0.41%	0.16%	0.72%	0.1%	0.41%	0.25%
1		2.03%	3.26%	4.02%	8.39%	0.14%	11.05%	1.66%	2.89%
2			0.05%	-	0.42%	-	-	0.5%	0.05%
3				-	0.89%	1.47%	-	0.86%	0.1%
4					1.33%	-	-	0.87%	0.35%
5						-	-	-	-
6							0.15%	6.83%	-
7								1.85%	0.74%
8									-

B Randomized smoothing for approximate certification

We measure the success of our attacks on approximate certification. We first provide background on how some of these mechanisms derive their guarantees and then present our experiments.

B.1 Background on randomized smoothing

Researchers have extensively studied approximate certification of non-linear models such as neural networks, under the L_2 norm [9, 8, 7]. In this work, we consider two such approaches due to Li *et al.* [8] and Cohen *et al.* [7] from which many subsequent results derive. Sufficiently stable model predictions lead to certifiable radii; therefore we seek to stabilize the outputs of the base classifier f by forming a smoothed classifier g as follows. To input $x \in \mathbb{R}^D$ add isotropic Gaussian noise, then apply f . The input distribution induces a distribution over predictions: output the most likely class. That is, for $\epsilon \sim \mathcal{N}(0, \sigma^2 I^2)$,

$$g(x) = \arg \max_{k \in [K]} \Pr(f(x + \epsilon) = k) .$$

Here hyperparameter $\sigma > 0$ controls the level of smoothing: higher values lead to larger radii and higher risk. Consider lower (upper) bounds on the winning k^* (runner-up) classification’s probability score, $\Pr(f(x + \epsilon) = k^*) \geq \underline{p}_A \geq \overline{p}_B \geq \max_{k \in [K] \setminus \{k^*\}} \Pr(f(x + \epsilon) = k)$. Then Cohen *et al.* prove that radius $R = 0.5\sigma(\Phi^{-1}(\underline{p}_A) - \Phi^{-1}(\overline{p}_B))$ is a sound certification for smoothed classification

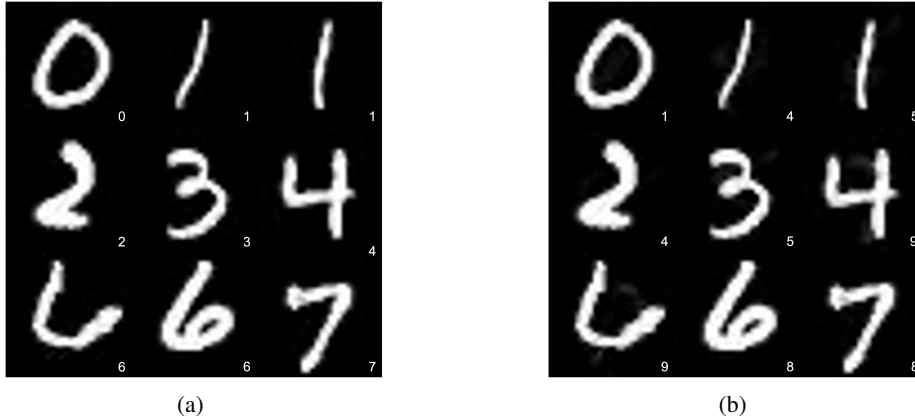


Figure 3: (a) Images of digits from the MNIST dataset. (b) Corresponding adversarial images that have changed the classifications of the LR model, with perturbation $\|\delta\| < R$. For example, the first image in (a) has certified radius $R = 93.82310999643202$, and is classified as 0, the corresponding adversarial image in (b) has perturbation $\|\delta\| = 93.82310999643201$, and is classified as 1. Labels at the bottom right of each image are the classifications of the LR model.

$g(x)$. Note the authors prove that when applied to linear classifiers, this R recovers the sound and complete radius above. Three challenges remain: (1) $g(x)$ can not be computed except for very simple classifiers like the linear classifier; (2) bounding the class probabilities; and (3) training for weights appropriate for low-risk classifications by $g(x)$ or its approximation, instead of $f(x)$. These challenges are addressed for non-linear models such as neural networks, by: (1) Form a Monte Carlo estimate of $g(x)$ by: take i.i.d. samples $\epsilon_1, \dots, \epsilon_M \sim \mathcal{N}(0, \sigma^2 I^2)$, then compute $\hat{g}(x) = \arg \max_{k \in [K]} \sum_{i=1}^M \mathbf{1}[f(x + \epsilon_i) = k]$. (2) Estimate a one-sided $(1 - \alpha)$ lower (Binomial) confidence interval in the case of $K = 2$ (a similar approach works more generally) to estimate $\underline{p}_A, \overline{p}_B$, and because this is using random $\hat{g}(x)$ we must estimate this interval using an additional much larger sample of $f(x + \epsilon)$, for small α . The resulting certification R is then sound with high probability $1 - \alpha$. (3) Ideally we would obtain parameters for $f(\cdot)$ for low-risk predictions with $\hat{g}(x)$ by fully evaluating this smoothed predictor per gradient update, however in practice we estimate this smoothed predictor with a single noise draw for computational efficiency.

B.2 Attack experiments on approximate certification

Our experiments on approximate certification are based on the MNIST [21] and the CIFAR10 [23] datasets, with the same network architecture and data preprocessing procedures as [4, 7]. All images are scaled to $[-0.5, 0.5]$, hence, all adversarial images must also stay in that range to avoid a trivial filter as a defense. We used C&W to find the perturbation direction in this attack. We did not use PGD because its success rate in finding an adversarial perturbation direction is much lower than that of C&W for the CIFAR-10 dataset.

Training. In order to classify noise-corrupted examples (*i.e.*, $\mathcal{N}(x, \sigma^2 I)$) correctly, we use the same Gaussian augmentation method as [7, 9] to train our models, across a set of parameters such as training noise scale $\sigma_T = \{0.5, 1.0\}$ and epoch number $E = \{20, 10\}$ for the CIFAR-10 dataset and MNIST dataset, respectively. We choose stochastic gradient descent (SGD), with momentum $m = 0.9$, as an optimizer to train our model, with batch size $B = 64$ and learning rate $l = 0.01$. Our CNN model’s validation accuracy for the MNIST dataset is 81.25%, and our ResNet20 model’s validation accuracy for the CIFAR-10 dataset is 50.0%. The validation accuracies on the MNIST and CIFAR-10 datasets are relatively low, due to the Gaussian noise added in the training and prediction processes.

Prediction and certified radius estimation. We adopt the same prediction procedures as [7] and [8]. Given an instance x , the smoothed classifier g runs the base classifier f on M noise-corrupted instances of x , and returns the top class k_A that has been predicted by f . The estimation of

Table 3: The attack success rates of C&W (adversarial examples outside of certified radius) and our rounding search (within the certified radius), evaluated two robust classifiers based on randomized smoothing: R_C [7] and R_L [8]. The number of Monte Carlo samples N used in certified radius estimation ranges in $\{100, 1000, 10000\}$. Train noise scale, σ_T , is 1.0 and 0.5 for the MNIST and the CIFAR-10 datasets, respectively. Predict noise scale $\sigma_P \in \{0.25, 0.5, 1.0\}$.

Dataset	σ_T	σ_P	N_g	C&W		Rounding search	
				attack rate		attack rate	
				R_C	R_L	R_C	R_L
MNIST	1.0	0.5	100	17.4%	18.3%	0.8%	0.7%
			1000	15.8%	15.0%	0.3%	0.3%
			10000	15.9%	15.5%	0.1%	0%
		1.0	100	26.1%	28.0%	1.3%	0.8%
			1000	26.1%	26.9%	0.3%	0.1%
			10000	24.8%	25.2%	0.1%	0.3%
CIFAR-10	0.5	0.25	100	4.5%	7.7%	0.8%	0.1%
			1000	4.7%	5.6%	1.0%	0.3%
			10000	4.0%	5.5%	1.0%	0%
		0.5	100	10.3%	9.9%	0.4%	0%
			1000	8.1%	6.5%	1.9%	0.1%
			10000	6.9%	5.9%	2.2%	0.1%

the certified radius for a smoothed classifier g is based on the probability distribution of the winner and runner-up classes (*i.e.*, p_A and p_B), for both R_C and R_L . p_A and p_B are estimated via interval estimation [27], with confidence $1 - \alpha$. We demand $p_A \geq p_B$ in the estimation of the certified radius, as in the Theorem 1 of [7]. As recommended in these papers, we set $\alpha = 0.1\%$, Gaussian prediction noise scale $\sigma_P \in \{0.25, 0.5, 1.0\}$, and let M range in $\{100, 1000, 10000\}$.

Attack. We adopt C&W attack as follows. Given x and R as returned by g , we run the the C&W attack against the base classifier f . Once C&W attack gives the perturbation and it is outside of the certified radius R , we scale the perturbation as in Equation (1), perform our rounding search from Section 3, and evaluate all generated adversarial examples using the robust classifier g . We chose not to use g in the process of perturbation generation as its stochastic nature makes looking for adversarial examples difficult as attacks based on gradients may not converge.

All adversarial examples must stay in their legal domain to ensure they can bypass a filter check on pixel values, and their perturbation norms must be smaller than the certified radius to ensure they would be certified. We randomly sample and evaluate $N = 10,000$ neighbors in the search area for each image.

We conduct attacks on 1,000 images of the MNIST and CIFAR-10 test datasets respectively, results are listed in Table 3. C&W has 0% attack success rate within R_C and R_L , so we did not list those results. Within R_C and R_L , our rounding attacks have up to 1.3% attack success rate on the MNIST dataset, and have up to 2.2% attack success rate on the CIFAR-10 dataset. An example of original and adversarial images are shown in Figures 4 and 5, together with their certified radii and perturbations.

Attack success rates within radius R_C are slightly higher than attack success rates within R_L , possibly due to the estimation method by Li *et al.* being more conservative than the one by Cohen *et al.* (See Figure 6.)

We note that one should consider above non-zero attack results carefully since both certified methods fall under approximate methods and have a failure rate of 0.1%. The goal of our experiments is to show that adversarial examples within R are possible and error rate should be reported and taken into account by practitioners when building systems that rely on these guarantees.

C Proof of Lemma 1

The result follows by strong induction on the levels of composition (equivalently levels of the computation tree) implementing $\underline{R}(f, x)$. The induction hypothesis is that up to $\ell \leq L$ levels of

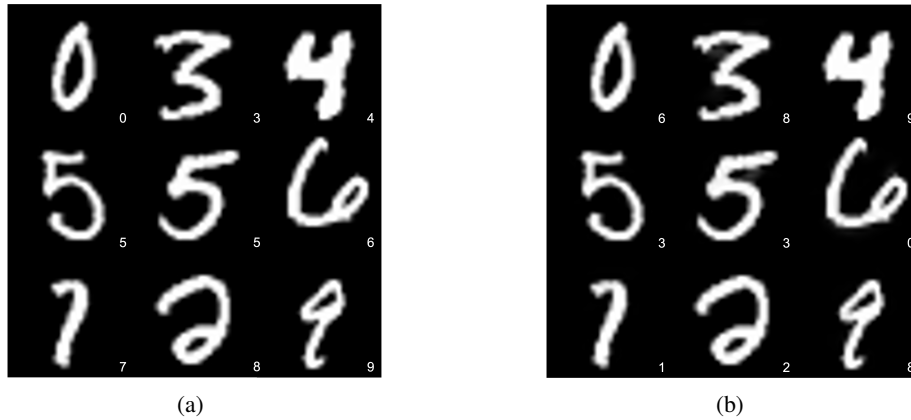


Figure 4: (a) Images of digits from the MNIST dataset. (b) Corresponding adversarial images that have changed the classifications of the CNN model, with perturbation $\|\delta\| < R$ [8]. For example, the second image in (a) has certified radius $R = 0.6343680620193481$, and is classified as 3, the corresponding adversarial image in (b) has perturbation $\|\delta\| = 0.6343680024147034$, and is classified as 8. Labels at the bottom right of each image are the classifications of the CNN model.

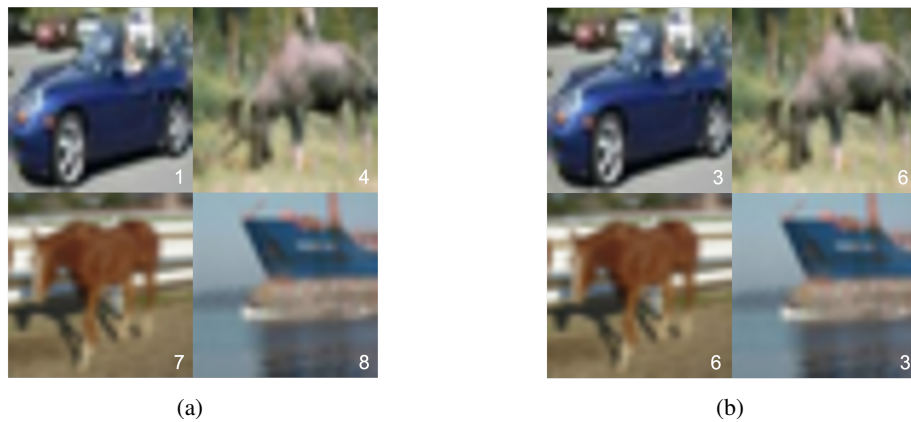


Figure 5: (a) Images from the CIFAR-10 dataset. (b) Corresponding adversarial images that have changed the classifications of the ResNet20 model, with perturbation $\|\delta\| < R$ [8]. For example, the first image in (a) has certified radius $R = 0.045056723058223724$, and is classified as 1, the corresponding adversarial image in (b) has perturbation $\|\delta\| = 0.045056719332933426$, and is classified as 3. Labels at the bottom right of each image are the classifications of the CNN model.

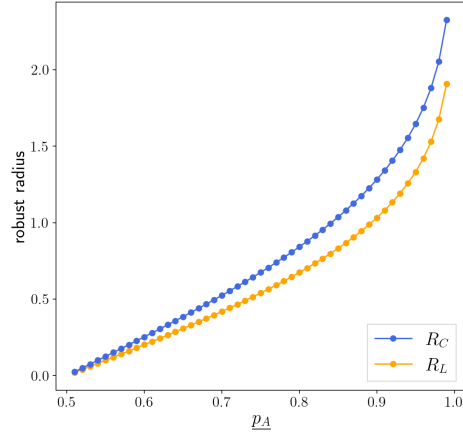


Figure 6: The distribution of R_C [7] and R_L [8]. The lower bound of the first class $\underline{p}_A \in [0.51, 0.99]$. The upper bound of the second class is set as $\overline{p}_B = 1 - \underline{p}_A$ in the estimation of R_C and R_L .

composition of interval operators produces intervals that contain the result of the corresponding real operators. The base case comes from the intervals $[x, x]$, $[f(x), f(x)]$ containing x , $f(x)$; the inductive step follows from repeated application of sound floating-point extensions.